Extra loss due to Fano resonances in inhibited coupling fibers based on a lattice of tubes

L. Vincetti* and V. Setti
Department of Information Engineering, University of Modena and Reggio Emilia, I-41125, Modena, Italy
**luca.vincetti@unimore.it*

Abstract: Confinement loss of inhibited coupling fibers with a cladding composed of a lattice of tubes of various shapes is theoretically and numerically investigated. Both solid core and hollow core are taken into account. It is shown that in case of polygonal shaped tubes, confinement loss is affected by extra loss due to Fano resonances between core modes and cladding modes with high spatial dependence. This explains why hollow core Kagome fibers exhibit much higher confinement loss with respect to tube lattice fibers and why hypocycloid core cladding interfaces significantly reduce fiber loss. Moreover it is shown that tube deformations, due for example to fabrication process, affect fiber performances. A relationship between the number of polygon sides and the spectral position of the extra loss is found. This suggests general guide lines for the design and fabrication of fibers free of Fano resonance in the spectral range of interest.

OCIS codes: (060.2400) Fiber properties; (060.4005) Microstructured fibers; (060.5295) Photonic crystal fibers.

References and links

1. F. Couny, F. Benabid, P. J. Roberts, P. S. Light, and M. G. Raymer, "Generation and photonic guidance of multi-octave optical-frequency combs," Science **318**, 1118–1121 (2007).
2. A. Argyros and J. Pla, "Hollow-core polymer fibers with a kagome lattice: potential for transmission in the infrared," Opt. Express **15**, 7713–7719 (2007).
3. T. Grujic, B. T. Kuhlmey, A. Argyros, S. Coen, and C. M. de Sterke, "Solid-core fiber with ultra-wide bandwidth transmission window due to inhibited coupling," Opt. Express **18**, 25556–25566 (2010).
4. A. D. Pryamikov, A. S. Biriukov, A. F. Kosolapov, V. G. Plotnichenko, S. L. Semjov, and E. M. Dianov, "Demonstration of a waveguide regime for a silica hollow-core microstructured optical fiber with a negatice curvature of the core boundary in the spectral region $> 3.5\mu m$," Opt. Express **19**, 1441–1448 (2011).
5. A. F. Kosolapov, A. D. Pryamikov, A. S. Biriukov, V. S. Shiryaev, M. S. Astapovich, G. E. Snopatin, V. G. Plotnichenko, M. F. Churbanov, and E. M. Dianov, "Demonstration of CO_2-laser power delivery through chalcogenide-glass iber with negativecurvature hollow core," Opt. Express **19**, 25723–25728 (2011).
6. J. Lu, C. Yu, H. Chang, H. Chen, Y. Li, C. Pan, and C. Sun, "Terahertz air-core microstructure fiber," Appl. Phys. Lett. **92**, 064105 (2009).
7. J. C. Travers, W. Chang, J. Nold, N. Y. Joly, and P. St. Russell, "Ultrafast nonlinear optics in gas-filled hollow-core photonic crystal fibers," J. Opt. Soc. Am. B **28**, A11–A26 (2011).
8. J. Anthony, R. Leonhardt, S. G. Leon-Saval, and A. Argyros, "THz propagation in kagome hollow-core microstructured fibers," Opt. Express **19**, 18470–18478 (2011).
9. S. Février, F. Gérôme, A. Labruyère, B. Beaudou, G. Humbert, and J. L. Auguste, "Ultraviolet guiding hollow-core photonic crystal fiber," Opt. Lett. **34**, 2888–2890 (2009).
10. L. Vincetti and V. Setti, "Confinement loss in kagome and tube lattice fibers: comparison and analysis," J. Lightwave Technol. **30**, 1470–1474 (2012).

#165684 - $15.00 USD Received 29 Mar 2012; revised 17 May 2012; accepted 30 May 2012; published 12 Jun 2012

11. L. Vincetti, V. Setti, and M. Zoboli, "Confinement loss of tube lattice and kagome fibers," in *Specialty Optical Fibers (SOF)* Toronto, Canada (2011).
12. Y. Y. Wang, N. V. Wheeler, F. Couny, P. J. Roberts, and F. Benabid, "Low loss broadband transmission in hypocycloid-core kagome hollow-core photonics crystal fiber," Opt. Lett. **36**, 669–671 (2011).
13. S. Février, B. Beaudou, and P. Viale, "Understanding origin of loss in large pitch hollow-core photonic crystal fibers and their design simplification," Opt. Express **18**, 5142–5150 (2010).
14. J. M. Stone, G. J. Pearce, F. Luan, T. A. Birks, J. C. Knight, A. K. George, and D. M. Bird, "An improved photonic bandgap fiber based on an array of rings," Opt. Express **14**, 6291–6296 (2006).
15. X. Jiang, T. G. Euser, A. Abdolvand, F. Babic, F. Tani, N. Y. Joly, J. C. Travers, and P. St. J. Russell, "Single-mode hollow-core photonic crystal fiber made from soft glass," Opt. Express **19**, 15438–15444 (2011).
16. L. Vincetti and V. Setti, "Waveguiding mechanism in tube lattice fibers," Opt. Express **18**, 23133–23146 (2010).
17. L. Vincetti and V. Setti, "Fano resonances in polygonal tube fibers," J. Lightwave Technol. **30**, 31–37 (2012).
18. U. Fano, "Effects of configuration interaction on intensities and phase shifts," Phys. Rev. **24**, 1866–1878 (1961).
19. S. Glasberg, A. Sharon, D. Rosenblatt, and A. A. Friesem, "Spectral shifts and line-shapes asymmetries in the resonant response of grating waveguide structures," Opt. Commun. **145**, 291–299 (1998).
20. S. S. Wang, R. Magnusson, J. Bagby, and M. G. Moharam, "Guided-mode resonances in planar dielectric-layer diffraction gratings," J. Opt. Soc. Am. A **7**, 1470–1474 (1990).
21. S. Fan, W. Suh, and J. D. Joannopoulos, "Temporal coupled-mode theory for the fano resonance in optical resonators," J. Opt. Soc. Am. A **20**, 569–572 (2002).
22. S. Fan and J. D. Joannopoulos, "Analysis of guided resonances in photonic crystal slabs," Phys. Rev. B **65**, 235112 (2002).
23. S. Selleri, L. Vincetti, A. Cucinotta, and M. Zoboli, "Complex FEM modal solver of optical waveguides with PML boundary conditions," Opt. Quantum Electron. **33**, 359–371 (2001).
24. S. L. Chuang, "A coupled mode formulation by reciprocity and a variational principle," J. Lightwave Technol. **5**, 5–15 (1987).
25. W. P. Huang and J. Mu, "Complex coupled-mode theory for optical waveguides," Opt. Express **17**, 19134–19152 (2009).
26. B. T. Kuhlmey, K. Pathmanandavel, and R. C. McPhedran, "Multipole analysis of photonic crystal fibers with coated inclusions," Opt. Express **14**, 10851–10864 (2006).
27. M. M. Z. Kharadly and J. E. Lewis, "Properties of dielectric-tube waveguides," Proc. IEEE **116**, 214–224 (1969).

1. Introduction

Inhibited Coupling Fibers (ICFs) have been extensively studied in recent years [1–9]. Their confinement mechanism is based on the inhibition of the coupling between the core and the cladding modes. When the coupling is high, then cladding becomes almost transparent to the electromagnetic wave, causing high confinement loss (CL). On the other hand, when the coupling is weak, the electromagnetic wave can propagate along the core with low loss [1, 2]. ICFs exhibit better performance than photonic band gap fibers in terms of low loss bandwidth and dispersion, but they suffer from higher loss. Reduction of loss in ICFs is thus a key point in the development of this kind of fibers. The microstructured cladding of ICFs is often composed of a regular arrangement of rods or tubes immersed in a background material. Tubes allow to obtain lower CL, larger transmission windows (TWs), and reduced bend sensitivity than rods [3–5]. For this reason, only Tube Lattice Fibers (TLF) will be considered in the following. Background material can be either air or a different dielectric material. In the first case, the fibers are known as Hollow Core TLFs (HC-TLFs), while in the second one as Solid Core TLFs (SC-TLFs). Kagome Fibers (KFs) belong to the group of HC-TLF since their microstructured cladding can be seen as composed of a regular arrangement of tubes with hexagonal shape [10]. KFs suffer from high confinement loss compared to HC-TLFs with circular tubes (Circular TLFs - CTLFs) [10, 11]. Numerical and experimental works have shown that this high confinement loss is connected to the shape of the core-cladding interface [12], and to the presence or absence of struts around the core [13]. The polygonal shape of the tubes composing the cladding of TLFs with both HC and SC can also be due to the drawing step of the fabrication process [2, 14, 15]. Recently, it has been numerically shown that in HC-TLFs with polygonal tubes (Polygonal TLFs - PTLFs), loss reduces by increasing the number of sides of the polygons, and that CTLFs exhibit the best performance [10]. The confinement loss in HC-TLFs seems thus

#165684 - $15.00 USD Received 29 Mar 2012; revised 17 May 2012; accepted 30 May 2012; published 12 Jun 2012

to depend on the shape of the struts composing the core boundary. However simple numerical results are not enough to fully understand the physical origin of this dependence and what are the fiber geometrical parameters that affect it.

The motivation of this paper originates from all these empirical observations, regarding both SC and HC-TLFs, and its goal is to develop a theoretical model able to fill this lack of knowledge, explaining the relationship between the cladding parameters and the confinement loss spectra in TLFs. A solid theoretical ground is of paramount importance as it provides useful information to find out possible ways to overcome the problem of high confinement loss in TLFs. The model here proposed is based on the observation that the confinement mechanism of TLFs can be fruitfully analyzed by starting from the analytical description of the modes of the tubes that compose their cladding [3,16]. When a stand alone Tube Fiber (TF) is perturbed, by changing its shape from circular to polygonal, confinement loss increases due to additional resonances [17]. These resonances exhibit an asymmetric shape typical of the Fano resonance. This kind of resonance was firstly observed in the context of solid state physics [18], and it has been more recently observed in a wide variety of optical structures such as microstructured fibers [3], gratings [19,20], and photonic crystals [21,22]. In TFs, these resonances occur between the core mode and some high order dielectric modes. The dielectric modes involved into the coupling mechanism are strictly related to the number of sides of the polygon.

In this paper it will be shown that a similar coupling mechanism also appears in TLFs when the tubes composing the cladding are changed from a circular shape (CTLFs) to a polygonal one (PTLFs). By applying the coupled mode theory to PTLFs, a simple analytical formula connecting the extra loss spectral regions to the number of sides is obtained. The higher the number of the sides of the tubes, the higher the frequencies where the extra losses appear. Circular shaped cladding tubes represent thus the best case for the confinement loss spectrum, while KFs composed of hexagonal tubes are affected by extra loss over the whole spectrum. This is very important both from a design and manufacturing point of view.

The numerical results shown in the paper are obtained through the modal solver COMSOL based on finite element method [23] and prove the validity of the model. At first, the analytical model is applied to a HC-TLF, explaining results reported in [10] and suggesting general manufacturing rules to reduce their confinement loss. The model is then applied also to a SC-TLF which have been presented in literature [14]. It is proved that the high confinement loss regions are due to the alteration of the cladding tube shape during the drawing process, and that a thorough control of the manufacturing process should allow better performance.

The paper is organized as follows. Section 2 shows the structure of both SC-TLFs and HC-TLFs considered in the analysis and it gives a brief overview of the confinement mechanism of TLFs. In the section 3 the relationship between extra loss and the tube shape is outlined through numerical results. The section 4 is devoted to the development of the analytical model based on the coupled mode theory. The model is validated in the section 5 through numerical results and comparison with experimental results reported in the literature. Conclusions follow.

2. Outline of the waveguiding mechanism in CTLFs

Figures 1(a) and 1(b) show the transverse cross sections that are typically used in CTLFs with HC and SC respectively [3, 6, 14, 16]. Claddings are composed of a regular arrangement of circular tubes with external radius R_c^{ext}, thickness t and refractive index n_1, separated by a pitch Λ and immersed in a uniform dielectric background with lower refractive index n_2. The cross section of a stand alone circular tube is reported in Fig. 1(c). In the HC-TLFs, the background material is air ($n_2 = 1$). The tubes must be in contact with each other and thus the tube radius R_c^{ext} and the pitch Λ are bounded each other. Kagome fibers can be seen as a particular case of these fibers in which tubes have an hexagonal shape [10]. In the SC-TLFs, the background

#165684 - $15.00 USD Received 29 Mar 2012; revised 17 May 2012; accepted 30 May 2012; published 12 Jun 2012

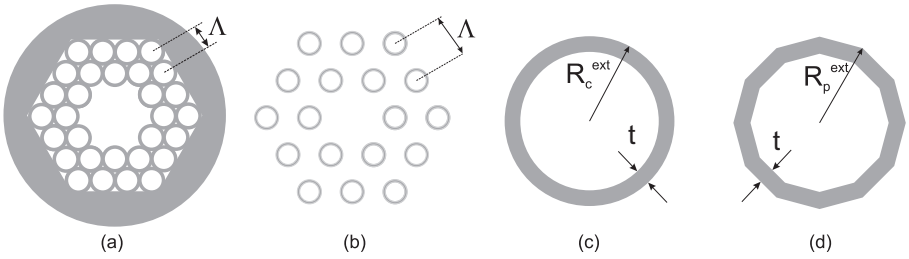

Fig. 1. (a)-(b) Cross sections of a HC-TLF and a SC-TLF respectively, with circular tubes in the cladding. (c)-(d) Cross sections of a standalone circular and a polygonal tube fiber. They also represent the tubes composing the cladding of CTLFs and PTLFs, respectively. White and gray regions represent low refractive index n_1 background material and high index n_2 one respectively.

material has a refraction index $n_2 > 1$. In this case, mechanical stability of the fiber is not a problem, thus Λ can have any desired value. Typically, for HC-TLFs also an external jacket that surrounds the cladding tubes is added in order to enhance the mechanical stability of the fiber structure. Its refractive index is here assumed to be equal to that of the cladding tubes for simplicity.

TLFs support three different kind of modes: core modes, which confine the major part of their electromagnetic power inside the core region; cladding hole modes (airy modes in HC-TLFs [2], [16]), which are confined in the inner part of cladding tubes; cladding ring modes, that concentrate their power mainly in the high index rings of the cladding tubes [16]. The first two kinds of modes have $n_{eff} < n_2$, whereas the latter has $n_2 \leq n_{eff} < n_1$. For the confinement mechanism purposes, only the core modes and the cladding ring modes can be considered. Cladding ring modes can be described in terms of a combination of the ring modes of the single tubes composing the cladding [3, 16] as shown in Figs. 2(a) and 2(b). In general, ring modes can be $HE^{ri}_{\xi,\gamma}$, $EH^{ri}_{\xi,\gamma}$, $TE^{ri}_{0,\gamma}$ and $TM^{ri}_{0,\gamma}$ modes. The subscripts ξ and γ, refer to the number of periods along the circumference direction of the tube and to the number of maxima/minima in the radial direction, respectively. In the SC-TLF usually $(n_2 - n_1)/n_2 << 1$ and ring modes can be described in terms of $LP^{ri}_{\xi,\gamma}$ modes which are composed of $HE^{ri}_{\xi+1,\gamma}$, $EH^{ri}_{\xi-1,\gamma}$ modes if $\xi \geq 2$. This approximation is no longer valid in HC-TLF because the step index is much higher. In this paper, for sake of simplicity, cladding ring modes are named after the ring modes composing them.

In order to introduce the general waveguiding properties of TLFs, SC-CTLFs will be considered, since the bigger Λ allows a clearer identification of the resonances with the cladding ring modes. A SC-CTLF with the cross section reported in Fig. 1(b), and a double layer of tubes around the core obtained by removing a tube is here considered [14]. The parameters are $n_1 = 1.47288$, $n_2 = 1.457$, $R_c^{ext} = 5.25\mu m$, $t = 472.5nm$, and $\Lambda = 15\mu m$. The bottom of Fig. 2(c) shows the confinement loss of the fundamental mode $HE^{co}_{1,1}$ versus the normalized frequency [1, 3]:

$$F = \frac{2t}{c} f \sqrt{n_1^2 - n_2^2} \tag{1}$$

where f and c are the frequency and the speed of light in vacuum, respectively. Confinement loss varies with frequency depending on the coupling between the core mode and the cladding ring ones [3, 16]. Such coupling depends on two factors: the difference between the effective indexes of core and ring modes, and the field integral overlap between them. The effect of the former is maximized at the crossing point between the dispersion curves of the two involved modes (phase-matching condition). Since the fibers work in the large core regime, the effective

#165684 - $15.00 USD Received 29 Mar 2012; revised 17 May 2012; accepted 30 May 2012; published 12 Jun 2012

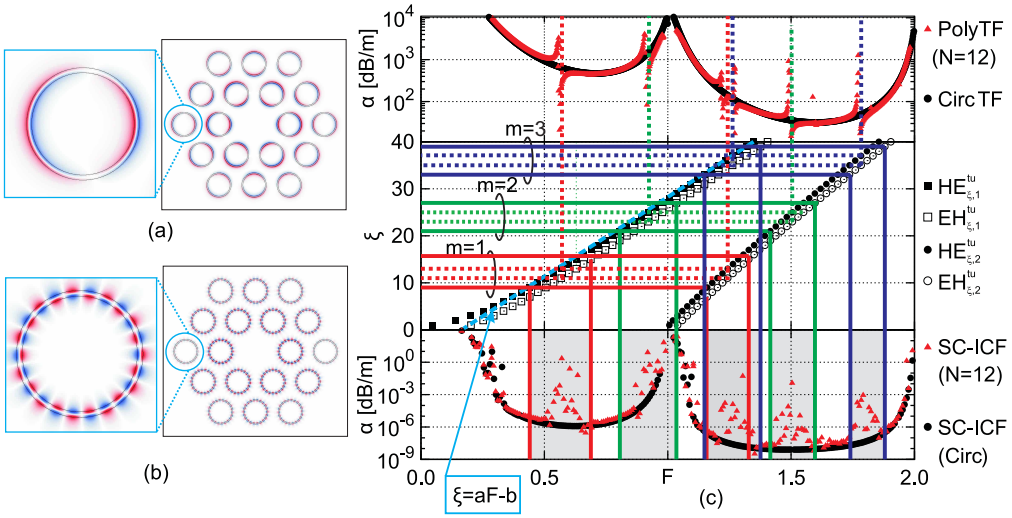

Fig. 2. (a)-(b) E_ϕ field component for the cladding ring modes $HE^{ri}_{1,2}$ and $LP^{ri}_{11,2}$ respectively. (c) Top: comparison of the confinement loss spectra of a circular (black dots) and a 12-sided polygonal (red triangles) tube fibers. Geometrical and physical properties of fibers are described through the paper. Middle: cutoff frequencies for the tube modes of the circular tube fiber. Dotted lines highlight the tubes modes which cause Fano resonances in tube fiber, according to Eq. (2). Solid lines highlight the cladding modes which defines the boundaries of the Fano resonances regions according to Eq. (8) with $\bar{\mu} = 3$. Red, green, and blue colors are used for the cases $m = 1$ and $m = 2$, respectively. Bottom: comparison of the confinement loss performance of SF-TLFs with circular (black dots) and 12-sided polygonal (red triangles) tubes in the cladding.

index of the core mode is very close to 1, thus the crossing frequencies can be well approximated by the cutoff frequencies of the ring modes [16, 17]. The modes overlap depends on spatial variation of the cladding ring modes along the tubes circumferences [1, 16]: the higher the periodicity, the lower the coupling. Figures 2(a) and 2(b) show the azimuthal field components of the electric field (E_ϕ) of two cladding ring modes with low and high spatial dependence, respectively. The former is the $LP^{ri}_{0,1} \leftrightarrow HE^{ri}_{1,1}$ mode which gives rise to high coupling with core mode at its cut-off frequency $F = 1$. The latter is the $LP^{ri}_{11,2}$ mode which is composed of $EH^{ri}_{10,2}$ and $HE^{ri}_{12,2}$ modes. Conversely to the previous one, its coupling with the core mode is weak because its spatial dependence along the tube boundary is high. For this reason, the confinement loss variation at its cut-off frequency $F = 1.54$ is negligible. As it will be shown in the next paragraph this is not longer true in TLFs composed of polygonal tubes.

3. Fano resonances in polygonal TFs and TLFs

The purpose of this section is to numerically show that, when the shape of the tubes change from circular to polygonal, extra loss appears in the confinement loss spectrum in both TFs and TLFs. The extra losses are due to the resonances between core mode and cladding modes with quickly spatial variation, which occur at the cut-off frequencies of the latter. As shown at the end of the previous paragraph, these couplings are absent in CTLFs. For sake of simplicity, only coupling with the fundamental mode $HE^{co}_{1,1}$ is here considered. These characteristics are highlighted by considering firstly a single polygonal TF (PTF) with solid core and then a SC-PTLF. Similar behaviors have been observed both in HC-PTFs [17] and in HC-PTLFs [10].

#165684 - $15.00 USD Received 29 Mar 2012; revised 17 May 2012; accepted 30 May 2012; published 12 Jun 2012

3.1. Polygonal tube fibers

The top of Fig. 2(c) compares confinement loss of a CTF and a PTF with $N = 12$ sides whose cross sections are reported in Figs. 1(c) and 1(d) respectively. Their parameters are the same as the tubes composing the cladding in the SC-TLFs considered in the previous section. Confinement loss spectrum of the PTF has some additional peaks due to extra-resonances. The peaks exhibit an asymmetric shape typical of the Fano resonance [18]. This behavior has already been found and analyzed in HC-TFs [17]. These additional resonances are due to the polygonal shape of the tube, which causes a coupling between the core and some ring modes with high azimuthal dependence. The ring modes involved in the coupling with the fundamental mode are the hybrid modes $HE_{\xi,\gamma}$ and $EH_{\xi,\gamma}$ with azimuthal index ξ:

$$|\xi - mN| = 1 \tag{2}$$

with m integer number.

In the SC-TF, being $n_2 - n_1 << 1$, the coupling strength is much lower and hybrid modes degenerate into linearly polarized modes: $LP^{ri}_{\xi,\gamma} \longleftrightarrow HE^{ri}_{\xi+1,\gamma}, EH^{ri}_{\xi-1,\gamma}$. Due to the weakness of the coupling, only $LP^{ri}_{mN,\gamma}$ modes give rise to non-negligible Fano resonances, because they are composed of hybrid modes both satisfying Eq. (2). In $LP^{ri}_{mN-1,\gamma}$ and $LP^{ri}_{mN+1,\gamma}$ modes, only one of the two hybrid modes satisfy Eq. (2), thus the resonances are much lower and they are not visible with the scale used in Fig. 2(c). A detail of the resonance with the $LP^{ri}_{12,1}$ mode is reported on the top of Fig. 3(a). Figure 3(b) clearly shows the hybridization between the core mode $HE^{co}_{1,1}$ and the ring $LP_{12,1}$ mode. In the middle of Fig. 2(c), the cut-off normalized frequencies of the ring modes $HE^{ri}_{\xi,\gamma}$ and $EH^{ri}_{\xi,\gamma}$ with $\gamma = 1, 2$ of a CTF are reported. Vertical dotted lines correspond to cut off of the $HE^{ri}_{mN+1,\gamma}$ and $EH^{ri}_{mN-1,\gamma}$ modes ($LP_{mN,\gamma}$) satisfying Eq. (2) with $m = 1$ (red lines), $m = 2$ (green lines), and $m = 3$ (blue lines). They coincide with Fano resonances in the confinement loss spectrum of the PTF.

3.2. Polygonal tube lattice fibers

Figure 2(c) compares confinement loss of the CTLF previously analyzed, and those of a PTLF composed of tubes with $N = 12$ sides. As in TFs, polygonal shapes cause a worsening of the confinement loss performance even if the peaks are spectrally wider. Figure 3(a) reports a detail of the loss in the spectral region $F \in [0.39, 0.75]$, showing that the widening is due to the resonance of the fundamental mode with a multiplicity of modes and not only with the $LP_{12,1}$ one. The same behavior holds for all the additional resonances, although they are not reported here for sake of brevity. In particular, it is found that the azimuthal index ξ of the resonant ring modes that couple to the core one is still strictly connected with N. The reason of the growth of the number of modes involved in the resonances with respect to TFs will be explained by the analytical model described in the next section and it is related to a much more complex core-cladding interface.

4. Analytical model

In order to investigate which cladding ring modes are able to couple to the core one, coupled mode theory is used [24, 25]. A PTLF with polygonal tubes in the cladding can be seen as the perturbed version of a CTLF. An example with $N = 6$ is shown in Fig. 4(a). A similar approach has already been successfully applied to investigate this kind of resonances in PTFs [17].

In TLFs, the overlap between ring and core modes is quite low and the coupling coefficient

#165684 - $15.00 USD Received 29 Mar 2012; revised 17 May 2012; accepted 30 May 2012; published 12 Jun 2012

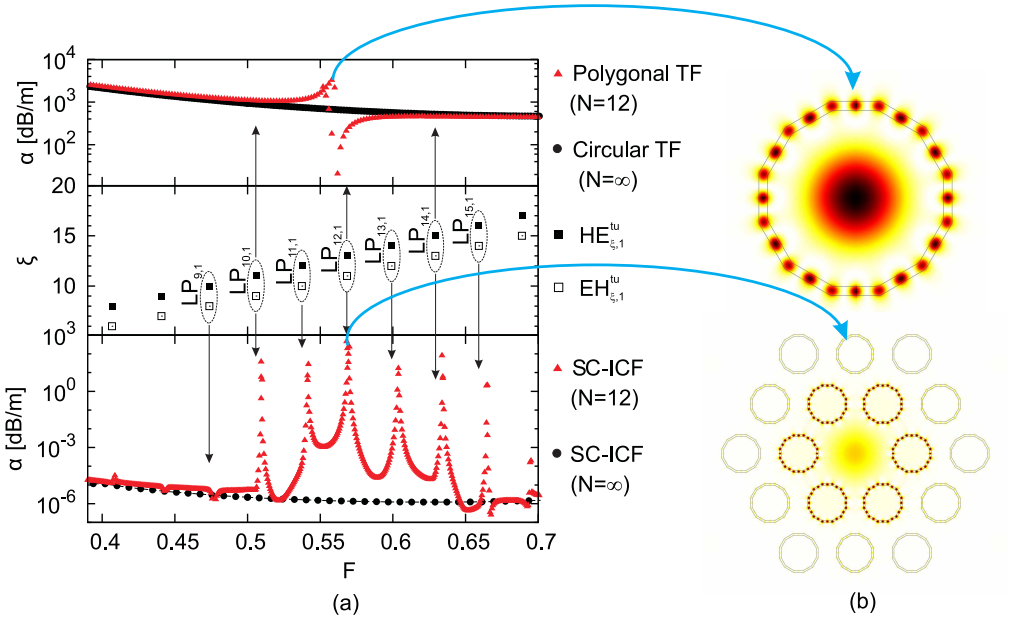

Fig. 3. (a) Zoom of Fig. 2(c) for $F = [0.39, 0.75]$. In the middle the degeneration of the $HE_{\xi+1,\gamma}$ and $EH_{\xi-1,\gamma}$ modes composing the $LP_{\xi,\gamma}$ modes is highlighted. (b) z-component of the Poynting vector of the guided mode at $F = 0.569373$ of the PTF (top) and PTLF (bottom) both with $N = 24$.

can be written as [17, 24]:

$$\tilde{K}_{co,ri} = \frac{\pi f}{2} \int\int_{S_\infty} \Delta\varepsilon \left(\bar{E}_t^{co} \cdot \bar{E}_t^{ri} - \frac{\varepsilon_c}{\varepsilon_c + \Delta\varepsilon} E_z^{co} E_z^{ri} \right) dS, \tag{3}$$

where S_∞ is the whole transverse plane, and the subscripts t and z indicate the transverse and longitudinal components of the electric field, respectively; ε_c is the dielectric permittivity of the CTLF, and $\Delta\varepsilon$ is the perturbation function shown in Fig. 4(a).

In order to find the conditions which guarantee that the integral (Eq. (3)) is non-zero, the N_t tubes composing the cladding are indexed by i and their centers are specified by vector $\bar{C}_i$ (see Fig. 4(a)). A local cylindrical coordinate system (r_i, ϕ_i) is introduced at the center of each cylinder. The perturbation function can thus be expressed as:

$$\Delta\varepsilon(\bar{r}) = \sum_{i=1}^{N_t} \Delta\tilde{\varepsilon}(\bar{r} - \bar{C}_i); \tag{4}$$

$\Delta\tilde{\varepsilon}$ is the perturbation of a PTF centered in the origin of the reference system (r, ϕ) and it is periodic along ϕ with period $2\pi/N$.

Due to the vectorial nature of the Eq. (3), its development gives rise to three similar integrals, one for each field component. By substituting Eq. (4) in each one of these integrals, it yields:

$$\tilde{K}^x_{co,ri} = (-1)^{\delta_{x,z}} \frac{\pi f}{2} \sum_{i=1}^{N_t} \int\int_{A_i} \Delta\tilde{\varepsilon} \left(\frac{\tilde{\varepsilon}_c}{\tilde{\varepsilon}_c + \Delta\tilde{\varepsilon}\,\delta_{x,z}} E_x^{co} E_x^{ri} \right) r_i \, d\phi_i \, dr_i \tag{5}$$

where $x = \{r, \phi, z\}$, $\delta_{x,z}$ is the Kronecker index, $\tilde{\varepsilon}_c$ is the permittivity of a CTF centered in the origin, and A_i is the surface where $\Delta\tilde{\varepsilon}(\bar{r} - \bar{C}_i) \neq 0$. Since cladding ring modes can be described

#165684 - $15.00 USD Received 29 Mar 2012; revised 17 May 2012; accepted 30 May 2012; published 12 Jun 2012

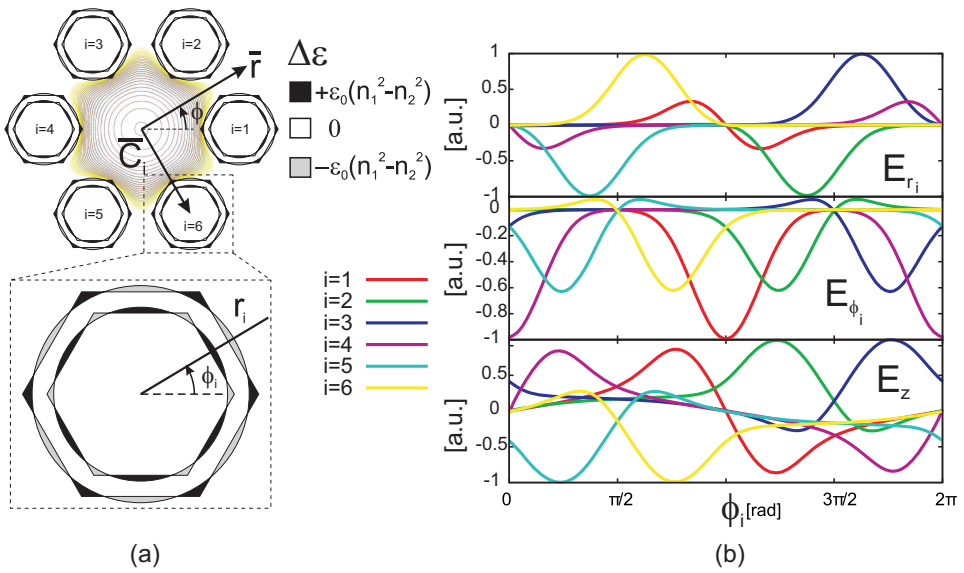

Fig. 4. (a) Example of perturbation function for a PTLF. z-component of the Poynting vector of the fundamental mode on log scale is also shown. The inset shows the perturbation function for a generic cladding tube, with the local reference system centered at its center. (b) Electric field components of the fundamental mode along the six innermost tubes of the TLF; different colors refer to different tubes.

as a composition of the modes of a CTF, in each integral of the series the field components of the ring modes can be expressed as [17]:

$$E_x^{ri}(r_i,\phi_i) = R_{x_1}^{ri}(r_i)\cos(\xi\phi_i) + R_{x_2}^{ri}(r_i)\sin(\xi\phi_i), \tag{6}$$

which are periodic functions with period $2\pi/\xi$ along ϕ_i. For the core modes, this is true in the TFs, but not in the TLFs as shown in Fig. 4(a), where the z component of the Poynting vector of the fundamental mode is reported on log scale. Despite that, since $\Delta\tilde{\varepsilon}(\bar{r}-\bar{C_i}) \neq 0$ only near the circular tube interface, E_x^{co} can be locally described by means of a Fourier-Bessel series [26]:

$$E_x^{co}(r_i,\phi_i) = \sum_{\mu=0}^{\bar{\mu}} A_{x\mu}R_{x_1}^{co,\mu}(r_i)\cos(\mu\phi_i) + B_{x\mu}R_{x_2}^{co,\mu}(r_i)\sin(\mu\phi_i), \tag{7}$$

where $\bar{\mu}$ is the integer at which the Fourier-Bessel series can be truncated without loss accuracy. As reported in Fig. 4(b), $\bar{E}^{co}$ components are slowly varying along ϕ_i with $i = 1,..,N_t$. This allows to consider very few terms in the series (Eq. (7)). By introducing Eq. (7) into Eq. (5), for each tube in the cladding there are $\bar{\mu}+1$ integrals equal to those of a PTF. For a PTF with N sides, a core mode with an azimuthal index $\tilde{\mu}$ couples with cladding modes with azimuthal index such that $|mN-\xi| = \tilde{\mu}$ [17]. In the TLF, all the harmonics of Eq. (7) must be considered and the condition on the ring modes becomes:

$$|mN-\xi| \leq \bar{\mu}. \tag{8}$$

In Fig. 2(c) solid lines correspond to cut-off of the $HE_{mN+1,\gamma}^{ri}$ and $EH_{mN-1,\gamma}^{ri}$ modes ($LP_{mN,\gamma}$) satisfying Eq. (8) with $\bar{\mu}=3$ and $m=1$ (red lines), $m=2$ (green lines), and $m=3$ (blue lines). They coincide with the edges of the high loss regions in the confinement loss spectrum of the PTLF.

#165684 - $15.00 USD Received 29 Mar 2012; revised 17 May 2012; accepted 30 May 2012; published 12 Jun 2012

In short, in TFs the core modes are described on the perturbation domain by only one sinusoidal function along the azimuthal direction. On the contrary, in the TLFs, the core modes do not exhibit a periodic trend on the perturbation. Despite that they can be described in terms of a series of periodic functions, each of which gives a non zero term to the integral (Eq. (3)). This justify the increment of the number of the resonances shown in Fig. 3(a).

It is important to point out that the model here developed does not rely on the particular perturbation, provided that it is a periodic function along the tube boundaries. As a consequence it can be also applied in case of non-polygonal deformation. Moreover, it does not rely on specific values of refraction indexes so it is valid for both SC-TLFs and HC-TLFs. The applicability to both kinds of fibers is shown in the next section.

4.1. Conditions to have a resonance free spectral region

The resonance having the lowest frequency F_q is the most important. It determines the spectral region $[0 : F_q]$ without Fano resonances, where confinement loss is very close to that of a CTLF [10, 17]. The first resonance is due to the $HE^{ri}_{N-\bar{\mu},1}$ mode. Cutoff frequencies of the modes of a TF are reported in the middle of Fig. 2(c). They are analytically known [27] and give a good approximation of those of the cladding ring modes. For every given F_q, it always exists a number of sides N which guarantee that resonance free spectral region. When $\xi >> 1$, the relationship between F^q and ξ is well approximated by:

$$\xi = aF - b. \tag{9}$$

Both the a and the b parameters depend on the geometrical and physical parameters of the cladding tubes. By combining Eq. (9) and (8) it yields:

$$F^q = \frac{N + b - \bar{\mu}}{a}, \tag{10}$$

thus the number of the sides N which guarantee the absence of Fano resonances in the spectral region $[0 : F_q]$ is:

$$N = \lceil aF^q - b + \bar{\mu} \rceil, \tag{11}$$

where $\lceil x \rceil$ denotes the nearest integer value that is bigger than x.

5. Numerical validation

5.1. HC-TLF

The HC-TLF here considered is shown in Fig. 1(a) with $R_c^{ext} = 5\mu m$, $t = 500nm$, $n_1 = 1.45$ and $n_2 = 1$. A single layer of tubes surrounds the HC obtained by removing the seven innermost ones. The parameters of the Eq. (9) are $a = 31.8$ and $b = 8$. The polygons in the cladding are oriented in such a way to contact each other only on vertices, as happens in the KFs [12, 13].

In Fig. 5(a) a polygonal HC-TLF with $N = 6$ is considered. It corresponds to a Kagome fiber with pitch $\Lambda = 9.5\mu m$ and strut thickness $t = 500nm$. Colored rectangles on the top of the graphs represent the cutoff regions of the rings modes that satisfy Eq. (8) with $\bar{\mu} = 3$. Different colors correspond to different values of the m parameter. Confinement loss is compared to that of a HC-CTLF. CLs coincide only in the high loss spectral regions corresponding to resonances with low azimuthal dependence ring modes [10, 16]. In the low loss regions, the Fano resonances due to hexagonal shape of the tubes composing the cladding cause a significant worsening of the confinement loss with respect to the circular case. Since $F^q = 0.24$ and the bands of $m = 1, 2, 3$ are partially overlapped, the Fano resonances cover the whole spectrum. Figure 5(b) shows the case of an HC-TLF with $N = 12$. The change from $N = 6$ to $N = 12$ shifts the

#165684 - $15.00 USD Received 29 Mar 2012; revised 17 May 2012; accepted 30 May 2012; published 12 Jun 2012

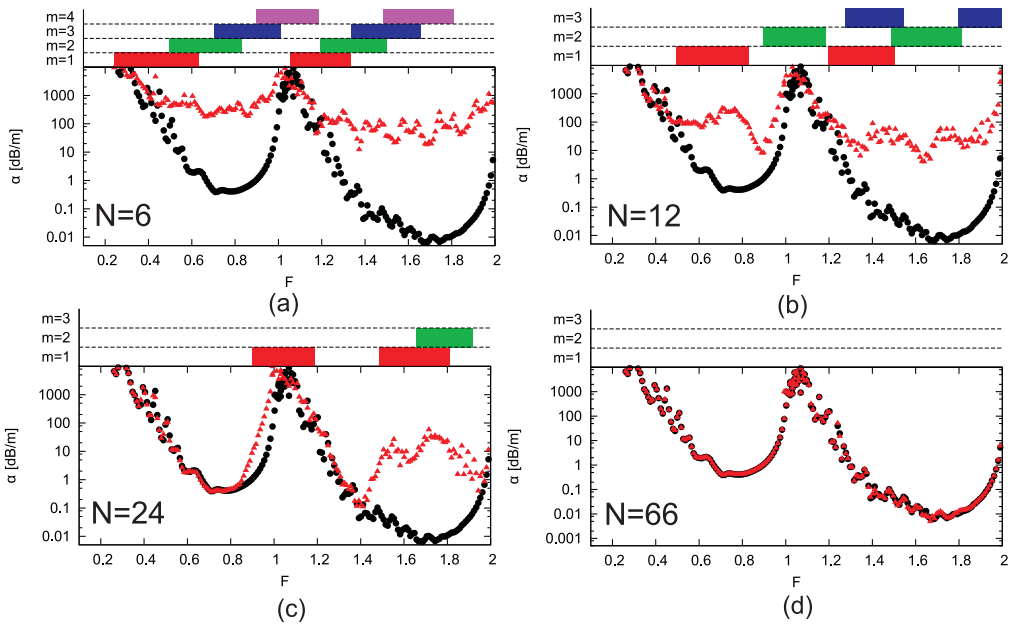

Fig. 5. Comparison of the confinement loss performances between a HC-TLF with circular (black dots) and N-sided polygonal HC-TLF (red triangles), with $N = 6$ (a), $N = 12$ (b), $N = 24$ (c), $N = 66$ (d). Rectangles on the top of the graphs represent the cutoff regions for the rings modes that satisfy Eq. (8) with $\overline{\mu} = 3$. Different colors are used for different values of the m parameter. In (a) only $m \leq 4$ has been considered for clearness.

bands toward higher frequencies, but $F^q = 0.53$ is still too low and the bands are still partially overlapped, thus there is not a significant improvement. By further increasing the sides up to $N = 24$ (Fig. 5(c)) an improvement of the confinement loss is obtained in the first and in the second transmission window. In fact, being $F^q = 0.91$, in the first transmission window there is a wide frequency range where confinement loss coincides with that of CTLF. Moreover, the bands with $m = 1$ and with $m = 2$ are no longer overlapped in the second transmission window creating a frequency range where confinement loss coincides with the circular case. For higher frequencies, there are still a lot of resonant modes that worsen the performance of the fiber. In order to widen the Fano resonance free region, polygons with a higher number of sides must be considered. From Eq. (11) by choosing $F^q = 2$, it yields $N \geq 62$. Actually $N = 66$ is required in order to satisfy geometrical constraints about the polygon vertices. Figure 5(d) shows the confinement loss performance for such fiber. As expected, the confinement loss performance of the 66-sided HC-PTLF remain very close to those of the HC-CTLF in the first two transmission windows.

Finally notice that the model and these results are in agreement with the results reported in [12] where the shape of the tubes facing towards the HC has been changed into a rounded one, obtaining a reduction of the CL.

5.2. SC-TLF

The model that have been developed through this paper is very useful to predict the effect of the manufacturing imperfections for both SC and HC-TLFs. For this purpose a SC-CTLF with $n_1 = 1.47288$, $n_2 = 1.457$, $t = 540nm$ and $R_c^{ext} = 5.4\mu m$ is taken into account [14]. As it can be seen in the scanning electron micrograph reported in [14], due to the manufacturing

#165684 - $15.00 USD Received 29 Mar 2012; revised 17 May 2012; accepted 30 May 2012; published 12 Jun 2012

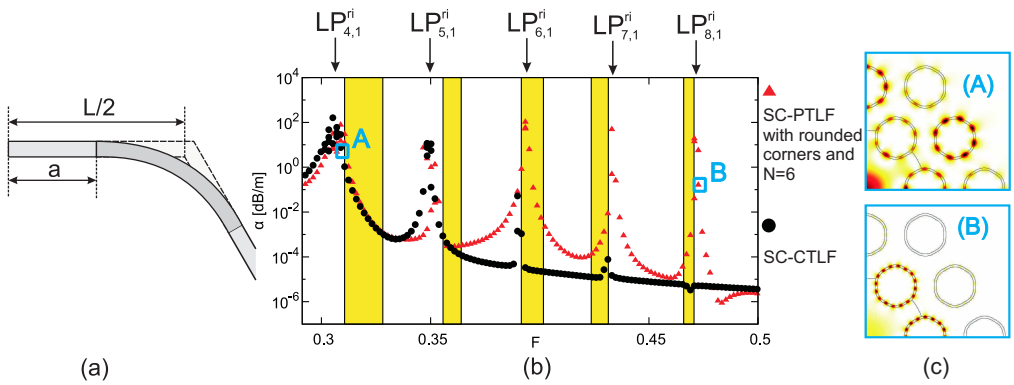

Fig. 6. (a) Rounding scheme of the polygon vertex: L is the length of the polygon side and a is the distance of the rounding point from the center of the side. (b) Comparison of the confinement loss between a SC-TLF with circles (black dots) or rounded hexagons (red triangles) in the cladding. Resonant rings modes are highlighted on the top of the figure. Yellow regions represent the high confinement loss regions reported in [14]. (c) Hybridization between core mode and ring modes $LP^{ri}_{4,1}$ (A) and $LP^{ri}_{8,1}$ (B) computed at $F = 0.305$ and $F = 0.47$, respectively.

process, cladding tubes are actually hexagons with rounded corners. Rounded corners do not affect the spectral position of the Fano resonances but reduce their bandwidth [17]. A smoothing parameter $s = 1 - 2a/L$, as shown in Fig. 6(a), is defined for the polygons of the cladding. In the simulations, $s = 0.75$ has been used. Figure 6(b) compares the confinement loss performance of the SC-PTLF with rounded hexagons with those of a SC-CTLF. Yellow regions represent the spectral regions with high transmission loss obtained experimentally in [14]. For the SC-CTLF, the resonance intensities with $LP^{ri}_{\xi,1}$ quickly decrease as ξ increases and the fiber does not exhibit high loss peaks for $F > 0.40$. On the contrary, the SC-PTLF exhibits all high loss peaks experimentally observed, showing that they are due to the hexagonal shape of the cladding elements. This is further confirmed by Fig. 6(c) which shows the modes found in simulations at $F = 0.305$ and $F = 0.47$. They agree with near field images reported in [14]. The differences of the spectral position of the loss peaks between numerical results and experimental ones are due to the fact that it was not possible to make a numerical prototype exactly like the fiber used in the experiment. For example, in the simulations the tube thickness was considered constant, whereas in the fabricated fiber the cross section of each tube is actually a ring of closely-spaced rods, spaced by around $0.6\mu m$, but the reported image does not allow to determine exactly their shape and size. A better agreement between numerical and experimental results can be obtained only by a higher resolution scanning micrograph image of the fiber cross section.

6. Conclusions

Confinement loss of inhibited coupling fibers with a cladding composed of a lattice of tubes of various shapes has been theoretically and numerically investigated. Both solid and hollow cores have been taken into account. It has been shown that in case of polygonal shaped tubes, confinement loss is affected by extra losses with respect to fibers with circular tubes. The extra losses are due to Fano resonances between core modes and cladding modes with high spatial dependence. By mean of a theoretical model based on the coupled mode theory, it has been shown that the spectral positions of the extra losses are intimately related to the number of sides of the polygonal tubes. The higher the number of sides, the higher their frequencies. Through

#165684 - $15.00 USD Received 29 Mar 2012; revised 17 May 2012; accepted 30 May 2012; published 12 Jun 2012

the model it has demonstrated that Kagome fibers are affected by extra loss over the whole transmission spectrum due to the small number of tube sides. This is the reason why Kagome fibers exhibit much higher confinement loss with respect to fibers made of circular tubes. The model has also allowed to demonstrate that some low transmission bands experimentally observed into solid core ICFs are due to the tube deformation occurred during the drawing step of the fabrication process. The developed model is thus a useful tool for inhibited coupling fibers, from both the design and the manufacturing point of view.

#165684 - $15.00 USD Received 29 Mar 2012; revised 17 May 2012; accepted 30 May 2012; published 12 Jun 2012